

## A simplified approach to the topology optimization of structures in case of unilateral material/supports

Matteo Bruggi<sup>1</sup>, Pierre Duysinx<sup>2</sup>

<sup>1</sup> Dept. of Civil and Environmental Engineering, Politecnico di Milano, Italy (matteo.bruggi@polimi.it);

<sup>2</sup> Dept. of Aerospace and Mechanical Engineering, University of Lige, Belgium (p.duysinx@ulg.ac.be)

### 1. Abstract

A simplified method to cope with the topology optimization of truss-like structures in case of unilateral behavior of material or supports is presented. The conventional formulation for volume-constrained compliance minimization is enriched with a set of stress constraints that enforce a suitable version of the Drucker-Prager strength criterion in order to prevent the arising of tensile (or compressive) members in the whole domain or within limited regions in the vicinity of the supports. The adopted numerical framework combines an ad hoc selection strategy along with the use of aggregation techniques that succeed in driving the energy-based minimization towards feasible designs through the enforcement of a limited number of stress constraints. Numerical simulations assess the proposed optimization framework in comparison with methods that are based on a full non-linear modeling of unilateral material/supports. An extension to the safety analysis of structures made of no-tension material is also highlighted.

**2. Keywords:** topology optimization, stress constraints, unilateral materials, unilateral supports, Drucker-Prager strength criterion.

### 3. Introduction

Most of the available formulations for topology optimization are conceived to cope with linear elastic structures exhibiting the same behavior in tension and compression for both material and ground constraints. Alternative formulations have been proposed in the recent literature to cope with tension-only or compression-only materials resorting to non-linear modeling, see e.g. [1], or to approaches mainly based on remodeling theories or material-replacement strategies that distribute the unilateral material depending on the stress flows directions in the design domain, see e.g. [2, 3, 4]. The assumption of unilateral behavior applies to boundary constraints in case of non-bilateral supports that provide a compressive reaction while being inactive in tension. A few methods have been proposed in the literature of structural optimization to address this particular class of problems and most of them resort to non-linear equations from contact mechanics, see e.g. [5, 6].

This contribution investigates the use of a simplified stress-based approach that is especially conceived to the optimal design of truss-like elastic structures in case of unilateral behavior of material or supports. The well-known volume-constrained minimization of compliance is endowed with a set of stress constraints that can efficiently control, all over the domain or along prescribed boundaries, the arising of bars with tension-only (or compression-only) strength. A smooth approximation of the no-tension (or no-compression) conditions governing the stress field is provided through the formulation of a suitable version of the Drucker-Prager strength criterion. An ad hoc strategy is implemented to robustly handle the arising multi-constrained formulation that is solved through mathematical programming. The adopted numerical framework combines the selection approach investigated in [7], along with the use of aggregation techniques, see e.g. [8, 9].

The presented numerical investigations point out that a limited set of constraints is needed in the first iterations of the optimization to steer the solution of the energy-driven optimization towards designs that take into full account the prescribed assumption of unilateral strength of material of supports. It is also shown that the proposed formulation may be adopted as a simplified but efficient tool for the preliminary safety analysis of structures that are made of no-tension material.

Numerical simulations confirms that the assumption of unilateral behavior of material/supports remarkably affects the achieved optimal design along with its structural performance. Non-trivial layouts can be obtained, depending on the design constraints.

### 4. Governing equations

The proposed formulation addresses the design of truss-like structures in case of unilateral material or

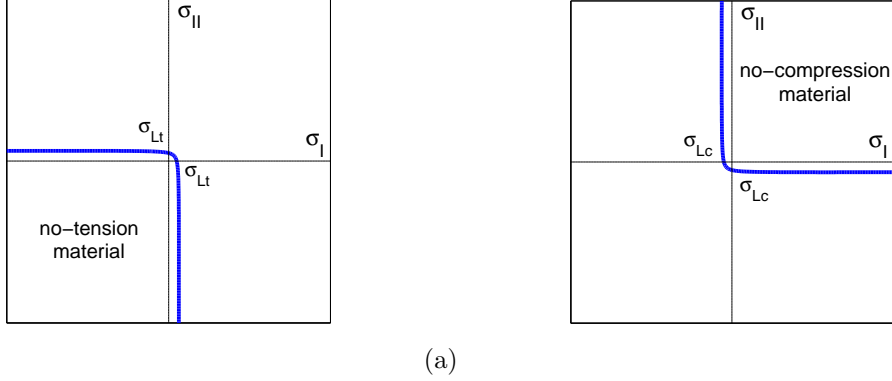


Figure 1: Unilateral materials: feasible domains defined by the Drucker–Prager strength criterion of Eqn. (5) in the plane  $\sigma_I$ – $\sigma_{II}$ . A prescribed small value of the tensile strength  $\sigma_{Lt}$  along with  $s = \sigma_{Lc}/\sigma_{Lt} = 100$  handles no–tension materials (a); a prescribed small value of the compressive strength  $\sigma_{Lc}$  along with  $s = \sigma_{Lc}/\sigma_{Lt} = 1/100$  handles no–compression materials (b).

constraints enforcing the non–symmetric behavior through a stress–based optimization. Such an approach moves from the governing equations that are found in conventional problems for minimum compliance.

Following the well–known SIMP model, see e.g. [10], one may introduce a suitable form of the fourth order elasticity tensor  $C_{ijhk}(\rho(\chi))$  depending on the local value of the density function  $\rho$ , i.e.:

$$C_{ijhk}(\rho(\chi)) = \rho(\chi)^p C_{ijhk}^0, \quad (1)$$

where  $C_{ijhk}^0$  is the stiffness tensor for a given isotropic medium, while  $p = 3$  is the penalization parameter assumed hereafter. Having the aim of formulating a two–dimensional problem of topology optimization for the stress–constrained maximization of the structural stiffness, the compliance is recalled as:

$$\mathcal{C} = \int_{\Omega} \rho^p C_{ijkl}^0 \varepsilon_{ij}(\underline{u}) \varepsilon_{kl}(\underline{u}) d\Omega, \quad (2)$$

where the strain tensor is defined as  $\varepsilon_{ij} = \frac{1}{2}(u_{i,j} + u_{j,i})$  in terms of the two–dimensional displacement field denoted as  $u_i$ . The stress field reads:

$$\sigma_{ij}(\underline{u}, \rho) = \rho^p C_{ijkl}^0 \varepsilon_{kl}(\underline{u}) = \rho^p \bar{\sigma}_{ij}(\underline{u}). \quad (3)$$

#### 4.1. Unilateral materials

Let consider the case of a unilateral material that has no tensile strength. Such an hypothesis requires the stress tensor  $\sigma_{ij}$  belong to the closed cone of negative semi–definite symmetric tensors, that is equivalent to restricting the principal stresses to be non–positive, see e.g. [11]. Within the two–dimensional framework, the following two inequalities hold all over the domain:

$$\sigma_{ii} \leq 0, \quad \sigma_{ii}\sigma_{jj} - \sigma_{ij}\sigma_{ij} \geq 0, \quad (4)$$

where  $\sigma_{ii}$  is the trace of the stress tensor, while  $\sigma_{ii}\sigma_{jj} - \sigma_{ij}\sigma_{ij}$  is twice the determinant. Alternatively, one may re–formulate the dual problem of no–compression material by simply requiring the stress tensor  $\sigma_{ij}$  belong to the closed cone of positive semi–definite symmetric tensors, i.e. changing the sign of Eqn. (4). The proposed approach is especially conceived to find optimal truss–like designs of minimum compliance stressed by uniaxial actions, while it can not be straightforwardly applied to structures governed by more complex bi–axial stress states. In such a case, the derivation of an ad hoc strain energy density function is required to perform the analysis and to compute the structural compliance of Eqn. (2), see e.g. [11].

Unilateral materials may be regarded as media having an extreme non–symmetric behavior in tension and compression. This straightforwardly suggests the adoption of a suitable form of the Drucker–Prager strength criterion [12] to handle a relaxed form of the relevant unilateral assumption, instead of dealing with the set of (non–smooth) Eqns. (4).

Let consider a material whose uniaxial strength in compression and tension are defined as  $\sigma_{Lc}$  and  $\sigma_{Lt}$ , respectively, being  $s = \sigma_{Lc}/\sigma_{Lt}$  the uniaxial asymmetry ratio. A stress state  $\sigma_{ij}$  belongs to the

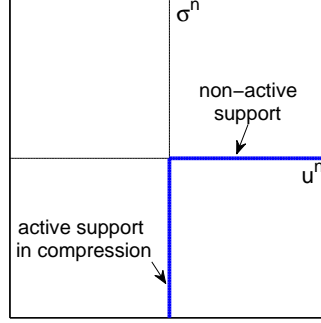


Figure 2: Unilateral supports: normal displacement  $u^n$  vs. normal stress–flux  $\sigma^n$  according to Eqns. (7).

feasible domain for the material strength if the following inequality on the equivalent stress measure  $\sigma^{eq}$  holds everywhere, see e.g. [7]:

$$\begin{aligned} \sigma^{eq} &= \alpha \sqrt{3J_{2D}} + \beta J_1 \leq 1, \\ \text{with } \alpha &= \frac{\sigma_{Lc} + \sigma_{Lt}}{2\sigma_{Lt}\sigma_{Lc}} \quad \text{and} \quad \beta = \frac{\sigma_{Lc} - \sigma_{Lt}}{2\sigma_{Lt}\sigma_{Lc}}, \end{aligned} \quad (5)$$

being  $J_1$  the first stress invariant of  $\sigma_{ij}$  and  $J_{2D}$  the second invariant of its deviatoric part, i.e.:

$$\begin{aligned} J_1 &= \sigma_{11} + \sigma_{22}, \\ 3J_{2D} &= \sigma_{11}^2 + \sigma_{22}^2 - \sigma_{11}\sigma_{22} + 3\sigma_{12}^2. \end{aligned} \quad (6)$$

The relevant admissible sets of stress states for a no–tension material is the third quadrant of the plane of the principal stresses  $\sigma_I$  and  $\sigma_{II}$ . Figure 1(a) shows that Eqn. (5) provides a smooth approximation of such a domain if a prescribed small value of the tensile strength  $\sigma_{Lt}$  along with  $s = \sigma_{Lc}/\sigma_{Lt} = 100$  is implemented.

No–compression materials stand in the first quadrant of the plane  $\sigma_I$ – $\sigma_{II}$ . Analogously, a prescribed small value of the compressive strength  $\sigma_{Lc}$  provides a smooth relaxation of the equations defining the first quadrant, i.e. the no–compression region, adopting  $s = \sigma_{Lc}/\sigma_{Lt} = 1/100$ , see Figure 1(b).

#### 4.2. Unilateral supports

A similar stress–based framework may be implemented to cope with unilateral behavior of ground constraints. Let consider unilateral supports that are prescribed along a portion of the boundary  $\Gamma_u$ , denoted as  $\Gamma_{uc}$ , with normal  $\underline{n}$ . The components of  $\underline{n}$  in the orthogonal reference frame are denoted as  $n_i$ , i.e.  $u^n = u_i n_i$  is the displacement along the normal, while  $\sigma^n = \sigma_{ij} n_i n_j$  is the normal component of the stress–flux across  $\Gamma_{uc}$ . Assuming no–tension support is equivalent to enforcing the following conditions along  $\Gamma_{uc}$ :

$$\begin{aligned} u_i n_i &= 0, \quad \sigma_{ij} n_i n_j \leq 0, \\ \text{or} \\ u_i n_i &\neq 0, \quad \sigma_{ij} n_i n_j = 0. \end{aligned} \quad (7)$$

Prescriptions of Eqns. (7) are represented in Figure 2, where admissible normal displacements  $u^n$  and relevant normal stress–flux  $\sigma^n$  are plotted. Alternatively, one may define a region of the two–dimensional domain that is adjacent to the boundary  $\Gamma_{uc}$ , namely  $\Omega_{uc}$ , and therein enforce the constraints used in case of no–tension materials, as introduced in Eqns. (4). This prevents the arising of tensile–stressed members that necessarily call for undesired tensile reactions along the boundary  $\Gamma_{uc}$ . Alternatively, more complex requirements on the behavior of ground constraints may be accomplished taking full account of the general equations for unilateral contact.

### 5. The optimization problem

As above introduced, suitable sets of stress constraints may be coupled to conventional equations to enforce a prescribed unilateral behavior of material or supports when seeking for optimal designs for volume–constrained maximum stiffness.

Both kinds of problems may be framed within the following discrete setting:

$$\left\{ \begin{array}{l} \min_{x_{min} \leq x_e \leq 1} \quad \mathcal{C} = \sum_{e=1}^N x_e^p \mathbf{U}_e^T \mathbf{K}_e^0 \mathbf{U}_e \\ \text{s.t.} \quad \sum_{e=1}^N x_e^p \mathbf{K}_e^0 \mathbf{U} = \mathbf{F}, \\ \sum_{e=1}^N x_e V_e \leq V_f \sum_{e=1}^N V_e, \\ x_i^{(p-q)} \bar{\sigma}_i^{eq} \leq 1, \quad \text{for } i = 1, \dots, N_a, \\ \left[ \frac{1}{N_c - N_a} \sum_{j=1}^{N_c - N_a} \left( x_j^{(p-q)} \bar{\sigma}_j^{eq} \right)^\eta \right]^{1/\eta} \leq 1, \end{array} \right. \quad (8)$$

that search for an optimal density distribution with element-wise constant component  $x_e$ , over a mesh of  $N$  four-node finite elements.

The objective function of the proposed formulation is the structural compliance  $\mathcal{C}$ , descending from the discretization of Eqn. (2) and computed from the element-wise contributions depending on the element density  $x_e$ , the displacement of its nodes  $\mathbf{U}_e$  and the local stiffness matrix for virgin material  $\mathbf{K}_e^0$ . Eqn. (8.2) is the discrete form of the equilibrium equation accounting for Eqn. (1), while Eqn. (8.3) is the constraint on the available amount of material. It requires the structural volume to be lower than a prescribed fraction  $V_f$  of the full domain, where  $V_e$  is the volume of the  $e$ -th element.

Aiming at an affordable and efficient enforcement of stress constraints, the adoption of a combined strategy of local and global handling is adopted, see Eqns. (8.4) and Eqn. (8.5). A suitable setting of the strength parameters in  $\bar{\sigma}_i^{eq}$  and  $\bar{\sigma}_j^{eq}$  allows coping with no-tension or no-compression conditions, according to the discussion reported in Section 4. In case of a structure made of unilateral material the stress field should be controlled all over the domain, while for unilateral behavior of the supports limited regions are considered. The number of constraints  $N_c$  is equal to  $N$  in the first case, while one has  $N_c \ll N$  if unilateral supports are dealt with.

Eqns. (8.4) refer to a suitable set of  $N_a$  local stress constraints enforced on the equivalent Drucker-Prager stress measure in the form of Eqn. (5). Following the strategy implemented in [7], a variable threshold increasing from 0,65 to 0,85 is adopted to select the left hand side of the set of  $N_a$  active stress constraints at each step of the optimization. To avoid any loss of convergence due to the variations of the set during the optimization procedure, the remaining  $N_c - N_a$  constraints are aggregated within the  $\eta$ -mean global enforcement of Eqn. (8.5), herein implemented with  $\eta = 6$  (see [13]).

To overcome the well-known *singularity problem* both set of constraints in Eqns. (8.4) and Eqn. (8.5) are relaxed through the adoption of the  $qp$ -approach, meaning that an exponent  $q < p$  is implemented to provide a strong relaxation in the low density region without introducing any remarkable bias at full density, see e.g. [14]. Following [7], the simulations presented next assume  $q = 2.5$ . Reference is also made to [15] for details on a previous application of the  $qp$ -approach to the global constraint of Eqn. (8.5).

A density filter is also implemented against mesh dependence and checkerboard issues, see e.g. [10], as already tested in the stress-based optimization proposed by [8].

The problem is solved via mathematical programming, adopting the Method of Moving Asymptotes by [16]. The enforcement of a lower bound  $x_{min} > 0$  is required on each density unknown  $x_e$  to avoid singularity of the equilibrium equation. The adopted gradient-based algorithm calls for the computation of sensitivity information that may be straightforwardly derived through the adjoint method.

## 6. Numerical simulations

The examples proposed in the sequel address results achieved in case of unilateral behavior of material, see Section 4.1, or unilateral behavior of supports, see Section 4.2. A material with Young modulus  $E = 1 \text{ N/m}^2$  and Poisson ratio  $\nu = 0.3$  is considered. The allowed volume fraction is  $V_f = 0.15$  for all the simulations.

The first example focuses on the geometry and boundary conditions defined in Figure 3(a), as similarly investigated by [17]. A rectangular domain is constrained by four hinges located at the corners and a downwards vertical force acts upon the center of the domain. A mesh of about 4000 elements is adopted to perform optimization on half of the lamina. Figure 4(a-b) presents the optimal design achieved by a

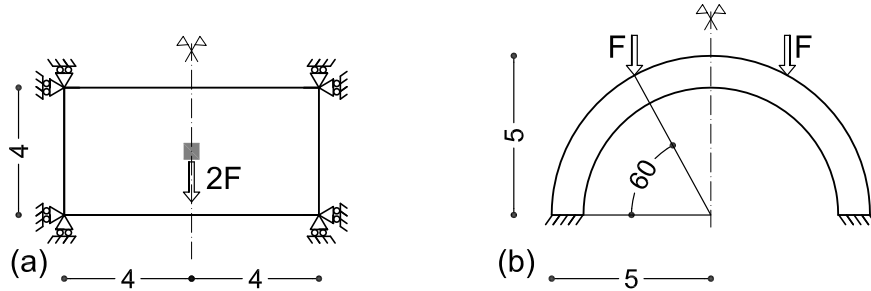


Figure 3: Example 1–2. Geometry and boundary conditions for the numerical applications (dimension in  $m$ , unitary thickness,  $F = 100 N$ ).

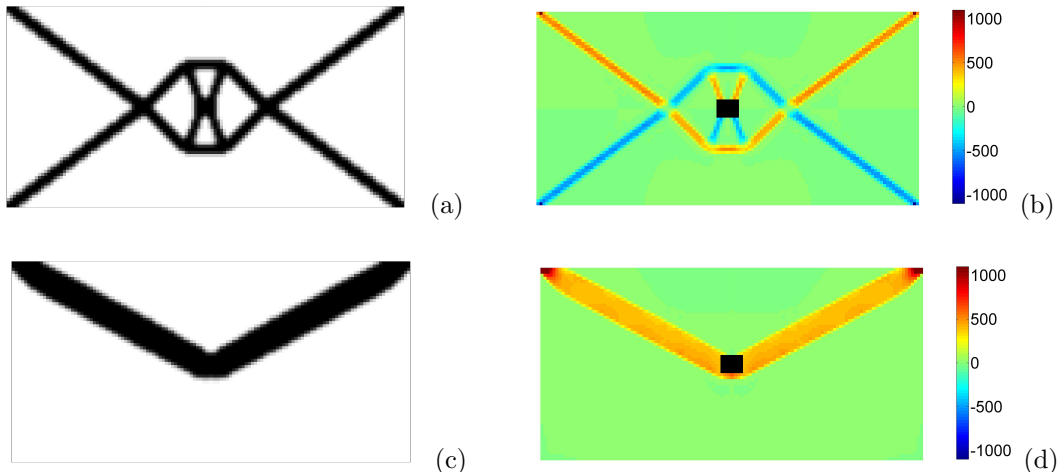


Figure 4: Example 1. Optimal design and relevant map of the first stress invariant: symmetric material (a–b), no-compression material (c–d).

conventional formulation for minimum compliance dealing with a material that has the same behavior in tension and compression. A map of the first stress invariant  $J_{1,e}$  is also provided to show that tensile and compressive stresses with modulus around  $800 N/m^2$  arise in the main truss-like members.

Figure 4(c–d) shows the optimal design achieved by the formulation in Eqn. (8), for a prescribed small value of the compressive strength  $\sigma_{Lc} = 50 N/m^2$  along with the assumption  $s = \sigma_{Lt}/\sigma_{Lc} = 100$ . The optimal truss-like structure consists of two thick ties connecting the load to the upper ground supports and no compressive member arises in the domain. The tensile-only layout does not exploit the supports located at the lower corners of the domain and one may wonder whether stress constraints simply prevent the optimizer from distributing material around these constrained regions. Figure 5(a–b) depicts the optimal result achieved by a pure volume-constrained minimum compliance formulation on the original problem, but removing the hinges located at the lower corners. As one may easily see the optimal design is not the same as that reported in Figure 4(c).

Figure 6(a) presents convergence curves of the non-dimensional compliance  $\mathcal{C}/\mathcal{C}_0$  for both the optimization problems solved in Figure 4. Subscript  $_0$  refers to the compliance computed on the full domain made of virgin material with symmetric behavior in tension and compression, assuming bilateral supports. In case of the pure volume-constrained compliance minimization a starting density that is equal to the allowed volume fraction is assigned, while full material values are assumed everywhere within the stress-based formulation of Eqn. (8). As investigated in [7] this allows reducing the amount of violated constraints at the beginning of the optimization, with a remarkable increase in terms of computational performance through the whole numerical procedure.

Looking at the records of the multi-constrained optimization one may observe that compliance grows in the first 15 – 20 steps, while it smoothly finds convergence in the remaining part of the diagram. Figure 6(b) shows that a number of stress constraints is active in the same first iterations; thereafter the procedure turns to a cheap volume-constrained optimization. Stress constraints drive the first steps of the procedure where they are able to steer the minimization towards the achievement of stiff designs that

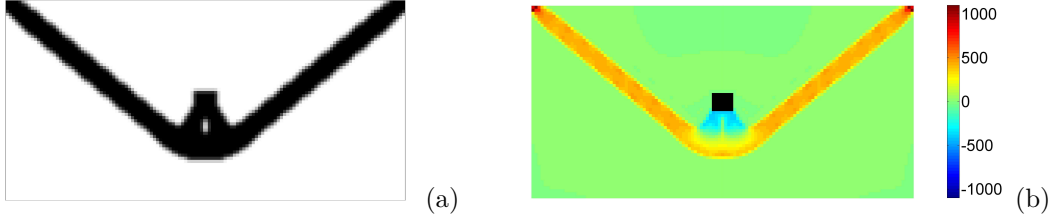


Figure 5: Example 1. Optimal design and relevant map of the first stress invariant in case of symmetric material and ground constraints active only at the upper corners of the domain.

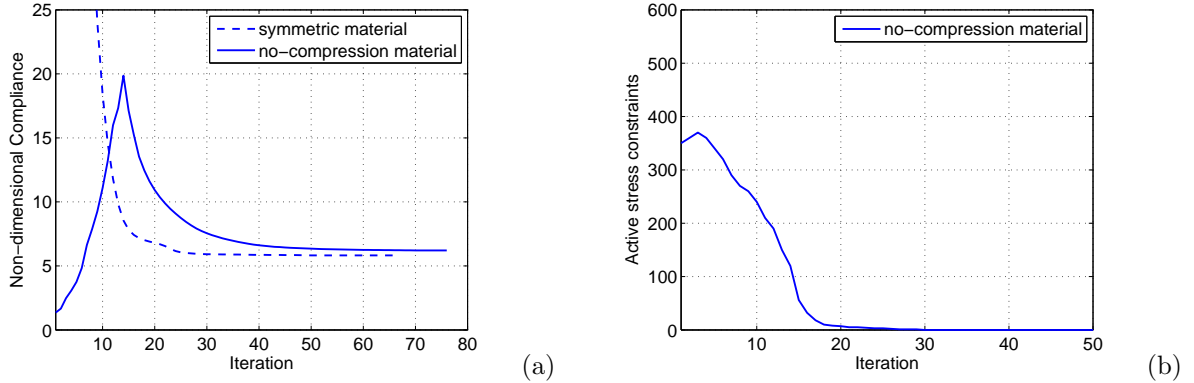


Figure 6: Example 1. Compliance convergence curves for the optimization problems solved in Figure 4 (a) and number of active stress constraints for the topology optimization with no-compression material (b).

are feasible with respect to the prescribed no-compression assumption.

An additional example concerns the arch-like structure made of no-tension material that is represented in Figure 3(b). A classical method to cope with the analysis and design of such kind of structures is based on the derivation of the so-called “line of thrust”, that is the funicular polygon made of the resultants of the compressive forces acting on each section of the arch. If the line of thrust falls within the thickness of the arch an equilibrium state can be found that is feasible with the no-tension assumption. Therefore, if the material has enough compressive strength, the structure is safe against collapse. Volume-constrained compliance minimization is used to derive strut-and-tie models that show the load path in elastic structures with symmetric behavior in tension and compression. The stress-constrained formulation of Eqn. (8) generates compression-only optimal design that may be therefore interpreted as strut-only load path for the structure. Figure 7 shows the line of thrust of the arch that has been obtained through topology optimization.

As detailed in Section 4.2, the formulation in Eqn. (8) may address unilateral supports enforcing stress constraints within limited regions that are adjacent to some relevant boundaries. The rectangular cantilever presented in Figure 8 is considered, including two regions of thickness  $w$  to provide a discretization of the zones connecting the horizontal edges of the cantilever to a rigid stand. Figure 9(a-c) shows the optimal design in case of bilateral supports along with the relevant stress maps for a vertical downwards or upwards force respectively, i.e.  $F_d$  or  $F_u$ . Tensile and compressive stresses with modulus around  $500 \text{ N/m}^2$  arise in the main truss-like members.

The same problem may be tackled by means of the formulation in Eqn. (8) to address the design in case of unilateral supports. This is done through the adoption of a set of stress constraints enforced within the two regions of thickness  $w$ , setting  $\sigma_{Lt} = 50 \text{ N/m}^2$  along with  $s = \sigma_{Lc}/\sigma_{Lt} = 100$ . Different layouts arise, depending on the sign of the applied load as presented in Figure 10(c-d). In both cases tensile reactions are straightforwardly avoided by preventing the minimizer to deploy ties along the supports. The achieved results are in good agreement with the work of [18] that originally investigated a contact problem between a cantilever of similar geometry and an outer elastic body.

Figure 11 presents convergence curves of the non-dimensional compliance  $C/C_0$  comparing the optimization problems solved in Figure 9. The same comments reported for Figure 6(a) apply to this

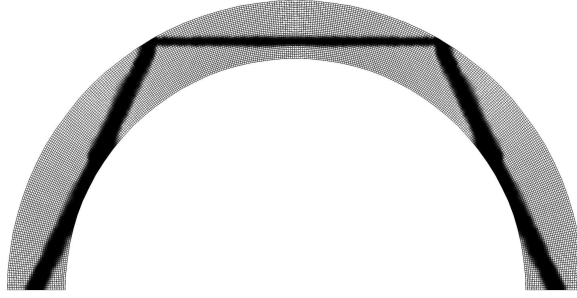


Figure 7: Example 2. The compression-only optimal design provides the “line of thrust” for the no-tension arch.

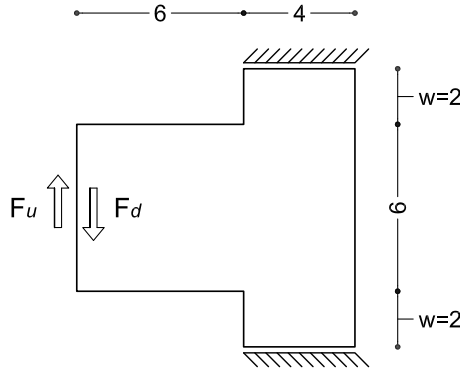


Figure 8: Example 3. Geometry and boundary conditions for the numerical applications (dimension in  $m$ , unitary thickness,  $F_d = F_u = 100 N$ ).

discussion. A few stress constraints enforce the required unilateral behavior in the very first steps of the procedure, while most of the optimization is performed as a pure volume-constrained minimization.

## 7. Conclusions

A simplified stress-based approach has been presented to address the optimal design of truss-like elastic structures in case of unilateral behavior of material or supports. The method consists in coupling the conventional volume-constrained compliance minimization with a set of local and global constraints that control the sign of the stresses arising in the achieved layout through the adoption of a suitable form of the Drucker-Prager failure criterion.

If unilateral material is dealt with, the optimal design is tackled enforcing constraints all over the domain. In case of unilateral supports, the stress regime is controlled within limited areas located in the vicinity of the ground constraints. In both cases a selection strategy is implemented to enforce local constraints on a small set of active elements while the remaining enforcements are aggregated within an additional global constraint. No additional modification is required to handle the inherent non-linearity of the considered problems.

Numerical simulations assess the proposed method comparing results with benchmarks of the recent literature. They also show that the proposed formulation may be adopted as a simplified but efficient tool for the preliminary analysis of structures that are made of no-tension (or no-compression) material, since an equilibrated load path may be interpreted as a possible “line of thrust” for the considered structural element.

The assumption of unilateral behavior of material/supports remarkably affects the achieved optimal design along with its structural performances.

## 8. References

- [1] C.J. Chang, B. Zheng, H.C. Gea, Topology optimization for tension/compression only design. *Proc.*

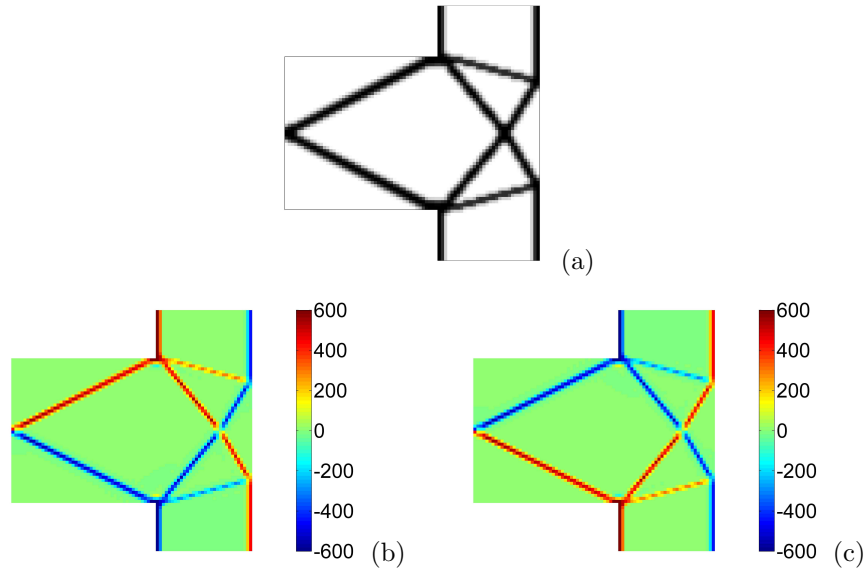


Figure 9: Example 3. Optimal design(a) and relevant map of the first stress invariant in case of bilateral supports under the action of  $F_d$ (b) or  $F_u$ (c).

of the 7th WCSMO, COEX Seoul, Korea, 2488-2495, 2007.

- [2] H. Guan, G.P. Steven, Y.M. Xie, Evolutionary structural optimisation incorporating tension and compression materials. *Adv Struct Eng* 2:273–288, 1999.
- [3] Q.M. Querin, M. Victoria, P. Marti, Topology optimization of truss-like continua with different material properties in tension and compression. *Struct Multidiscip Optim* 42:2532, 2010.
- [4] K. Cai, A simple approach to find optimal topology of a continuum with tension-only or compression-only material. *Struct Multidiscip Optim* 43:827-835, 2011.
- [5] E.A. Fancello, Topology optimization of minimum mass design considering local failure constraints and contact boundary conditions. *Struct Multidiscip Optim* 32:229-240, 2006.
- [6] N. Strmberg, A. Klarbring, Topology optimization of structures in unilateral contact. *Struct Multidisc Optim* 41:57-64, 2010.
- [7] M. Bruggi, P. Dusiynx, Topology optimization for minimum weight with compliance and stress constraints. *Struct Multidiscip Optim* 46:369-384, 2012.
- [8] C. Le, J. Norato, T.E. Bruns, C. Ha, D.A. Tortorelli, Stress-based topology optimization for continua. *Struct Multidiscip Optim* 41:605-620, 2010.
- [9] Y. Luo, M.Y. Wang, Z. Kang, An enhanced aggregation method for topology optimization with local stress constraints. *Comp Meth Appl Mech Eng* 254:31-41, 2013.
- [10] M.P. Bendsøe, O. Sigmund, Topology optimization - Theory, methods and applications, Springer, EUA, New York, 2003.
- [11] G. Del Piero, Constitutive equation and compatibility of the external loads for linear elastic masonry-like materials. *Meccanica* 24:150–162, 1989.
- [12] D.C. Drucker, W. Prager, Soil mechanics and plastic analysis or limit design. *Quart Appl Math* 10:157–165, 1952.
- [13] P. Dusiynx and O. Sigmund, New developments in handling stress constraints in optimal material distribution. *Proc. of the Seventh Symposium on Multidisciplinary Analysis and Optimization*, AIAA-98-4906, 1501-1509, 1998

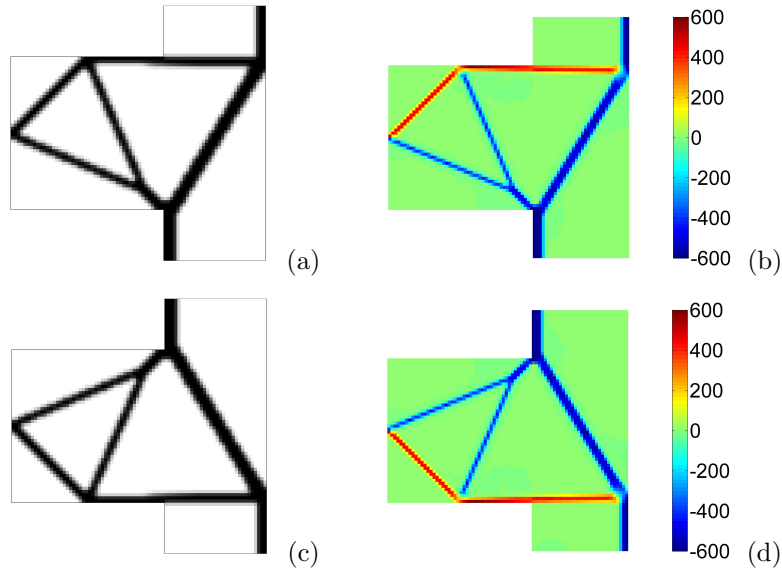


Figure 10: Example 3. Optimal design and relevant map of the first stress invariant in case of unilateral supports under the action of  $F_d$ (a–b) or  $F_u$ (c–d).

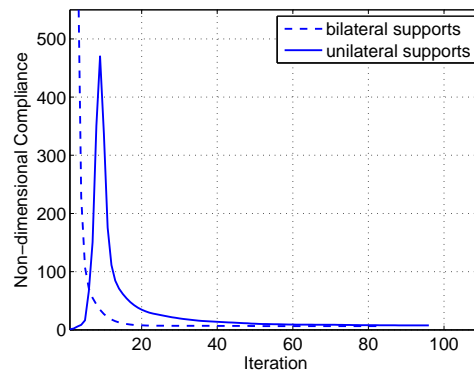


Figure 11: Example 3. Compliance convergence curves for the optimization problems solved in Figures 9 and 10.

- [14] M. Bruggi, On an alternative approach to stress constraints relaxation in topology optimization. *Struct Multidiscip Optim* 36:125–141, 2008.
- [15] M. Bruggi, P. Duysinx, On the use of a truly-mixed formulation in topology optimization with global stress-constraints. *Proc. of the 8th WCSMO*, Lisbon, Portugal, 2009.
- [16] K. Svanberg, Method of moving asymptotes - A new method for structural optimization. *Int J Numer Methods Eng* 24:359–373, 1987.
- [17] K. Cai, J. Shi, Z.Z. Wang, Tension/compression-only optimal stiffness design with displacement constraint. *Proc. of the 2010 Int Conf on Intelligent Computation Technology and Automation*, Changsha, China, 678–681, 2010.
- [18] N. Strömberg, Topology optimization of two linear elastic bodies in unilateral contact. *Proc. of the 2<sup>nd</sup> Int Conf on Engineering Optimization*, Lisbon, Portugal, 2010.